Charmonium levels near threshold and the narrow state $X(3872)\to\pi^+\pi^- J/\psi$

Estia J. Eichten*
Theoretical Physics Department, Fermi National Accelerator Laboratory, P.O. Box 500, Batavia, Illinois 60510, USA

Kenneth Lane†
Department of Physics, Boston University, 590 Commonwealth Avenue, Boston, Massachusetts 02215, USA

Chris Quigg‡
Theoretical Physics Department, Fermi National Accelerator Laboratory, P.O. Box 500, Batavia, Illinois 60510, USA
(Received 28 January 2004; published 24 May 2004)

We explore the influence of open-charm channels on charmonium properties and profile the 1^3D_2, 1^3D_3, and 2^1P_1 charmonium candidates for $X(3872)$. The favored candidates, the 1^3D_2 and 1^3D_3 levels, both have prominent radiative decays. The 1^3D_2 might be visible in the $D^0\overline{D}{}^{*0}$ channel, while the dominant decay of the 1^3D_3 state should be into $D\overline{D}$. We propose that additional discrete charmonium levels can be discovered as narrow resonances of charmed and anticharmed mesons.

DOI: 10.1103/PhysRevD.69.094019 PACS number(s): 14.40.Gx, 13.25.Gv, 14.40.Lb

I. INTRODUCTION

Encouraged by the Belle Collaboration's sighting [1] of $\eta_c'(2^1S_0)$ in exclusive $B\to KK_SK^-\pi^+$ decays, we sketched a coherent strategy to explore η_c' and the remaining charmonium states that do not decay into open charm, $h_c(1^1P_1)$, $\eta_{c2}(1^1D_2)$, and $\psi_2(1^3D_2)$, through B-meson gateways [2]. We argued that radiative transitions among charmonium levels and $\pi\pi$ cascades to lower-lying charmonia would enable the identification of these states.

Now the Belle Collaboration has presented evidence [3] for a new narrow state, $X(3872)\to\pi^+\pi^- J/\psi$, seen in $B^\pm\to K^\pm X(3872)$. The Collider Detector and Fermilab (CDF) Collaboration has confirmed the new state in inclusive 1.96-TeV $\overline{p}p\to X(3872)+$anything [4], as has the DØ experiment [5]. In addition, the CLEO [6], BaBar [7], and Belle [8] experiments have confirmed and refined the discovery of η_c', fixing its mass and width as $M(\eta_c')=3637.7\pm4.4$ MeV and $\Gamma(\eta_c')=19\pm10$ MeV [9].

In this article, we develop the hypothesis that $X(3872)$ is a charmonium level. The new meson's position at $D^0\overline{D}{}^{*0}$ threshold makes it imperative to take account of the coupling between $c\overline{c}$ bound states and open-charm channels. Accordingly, we revisit the properties of charmonium levels, using the Cornell coupled-channel model [10,11] to assess departures from the single-channel potential-model expectations. Far below the charm threshold, the nonrelativistic potential model is a good approximation to the dynamics of the charm-anticharm system. For excited states above the first few levels, the coupling of $c\overline{c}$ to charmed-meson pairs modifies wave functions, masses, and transition rates. We estimate spin splittings induced by communication with open-charm channels and examine the effect of configuration mixing on radiative decay rates. We consider ψ_2 (1^3D_2), ψ_3 (1^3D_3), and h_c' (2^1P_1) as possible interpretations of $X(3872)$, commenting briefly on diagnostics of a general character that will help establish the nature of $X(3872)$. Independent of the identity of $X(3872)$, above-threshold charmonium states should be visible as narrow structures in $1^3D_3\to D\overline{D}$, $2^3P_2\to D\overline{D}$, $D\overline{D}{}^*$, $1^3F_4\to D\overline{D}$, $D\overline{D}{}^*$, and possibly $2^3P_0\to D\overline{D}$.

What do we know about $X(3872)$? Belle's clean sample of 36 events, entirely from B-meson decays, determines the mass of the new state as $3872.0\pm0.6\pm0.5$ MeV and yields a ratio of production×decay branching fractions,

$$\frac{\mathcal{B}(B^+\to K^+X)\mathcal{B}(X\to\pi^+\pi^-J/\psi)}{\mathcal{B}(B^+\to K^+\psi')\mathcal{B}(\psi'\to\pi^+\pi^-J/\psi)}=0.063\pm0.014. \quad (1)$$

CDF observes 730 ± 90 events above background and determines a mass $3871.4\pm0.7\pm0.4$ MeV. The observed mass lies 67 MeV above the 1^3D_J centroid in the potential-model template of Ref. [2]. The large number of events suggests that much of the CDF sample arises from prompt production of $X(3872)$, not from B decays, and opens another path to the exploration of new charmonium states. Belle sets a 90% C.L. upper limit on the width, $\Gamma(X(3872))<2.3$ MeV. The $\pi^+\pi^-J/\psi$ decay appears to favor high dipion masses, but there is no detailed information yet about the quantum numbers J^{PC}. Belle has searched in vain for radiative transitions to the 1^3P_1 level; their 90% C.L. upper bound,

$$\frac{\Gamma(X(3872)\to\gamma\chi_{c1})}{\Gamma(X(3872)\to\pi^+\pi^-J/\psi)}<0.89, \quad (2)$$

conflicts with our single-channel potential-model expectations for the 1^3D_2 state [2]. The theoretical estimate of the $\pi\pi J/\psi$ rate is highly uncertain, however.

*Email address: eichten@fnal.gov
†Email address: lane@bu.edu
‡Email address: quigg@fnal.gov

TABLE I. Thresholds for decay into open charm.

Channel	Threshold energy (MeV)
$D^0\bar{D}^0$	3729.4
D^+D^-	3738.8
$D^0\bar{D}^{*0}$ or $D^{*0}\bar{D}^0$	3871.5
$D^\pm D^{*\mp}$	3879.5
$D_s^+D_s^-$	3936.2
$D^{*0}\bar{D}^{*0}$	4013.6
$D^{*+}D^{*-}$	4020.2
$D_s^+\bar{D}_s^{*-}$ or $D_s^{*+}\bar{D}_s^-$	4080.0
$D_s^{*+}D_s^{*-}$	4223.8

II. INFLUENCE OF OPEN-CHARM STATES

The Cornell group showed long ago that a very simple model that couples charmonium to charmed-meson decay channels confirms the adequacy of the single-channel $c\bar{c}$ analysis below threshold and gives a qualitative understanding of the structures observed above threshold [10,11]. We now employ the Cornell coupled-channel formalism to analyze the properties of charmonium levels that populate the threshold region between $2M(D)$ and $2M(D^*)$, for which the main landmarks are shown in Table I.

Our command of quantum chromodynamics is inadequate to derive a realistic description of the interactions that communicate between the $c\bar{c}$ and $c\bar{q}+\bar{c}q$ sectors. The Cornell formalism generalizes the $c\bar{c}$ model without introducing new parameters, writing the interaction Hamiltonian in second-quantized form as

$$\mathcal{H}_I=\frac{3}{8}\sum_{a=1}^{8}\int :\rho_a(\mathbf{r})V(\mathbf{r}-\mathbf{r}')\rho_a(\mathbf{r}'):d^3r\,d^3r', \qquad (3)$$

where V is the charmonium potential and $\rho_a(\mathbf{r})=1/2\psi^\dagger(\mathbf{r})\lambda_a\psi(\mathbf{r})$ is the color current density, with ψ the quark field operator and λ_a the octet of SU(3) matrices. To generate the relevant interactions, ψ is expanded in creation and annihilation operators (for charm, up, down, and strange quarks), but transitions from two mesons to three mesons and all transitions that violate the Zweig rule are omitted. It is a good approximation to neglect all effects of the Coulomb piece of the potential in Eq. (3).

A full outline of the calculational procedure appears in Refs. [10,11], but it is apt to cite a few elements here. We evaluate Eq. (3) between nonrelativistic $(c\bar{c})$ states with wave functions determined by the Cornell potential and 1^1S_0 and 1^3S_1 $c\bar{u}$, $c\bar{d}$, and $c\bar{s}$ ground states with Gaussian wave functions. States with orbital angular momentum $L>0$ can decay in partial waves $\ell=L\mp1$.

Following [10], we define a coupling matrix within the $(c\bar{c})$ sector

$$\Omega_{nm}(W)=\sum_{ij}\frac{\langle n|\mathcal{H}_I|D_i\bar{D}_j\rangle\langle D_i\bar{D}_j|\mathcal{H}_I|m\rangle}{(W-E_{D_i}-E_{\bar{D}_j}+i\varepsilon)}, \qquad (4)$$

TABLE II. Statistical recoupling coefficients C, defined by Eq. (D19) of Ref. [10], that enter the calculation of charmonium decays to pairs of charmed mesons. Paired entries correspond to $\ell=L-1$ and $\ell=L+1$.

State	$D\bar{D}$	$D\bar{D}^*$	$D^*\bar{D}^*$
$^1S_0$	$-:0$	$-:2$	$-:2$
$^3S_1$	$-:\frac{1}{3}$	$-:\frac{4}{3}$	$-:\frac{7}{3}$
$^3P_0$	1:0	0:0	$\frac{1}{3}:\frac{8}{3}$
$^3P_1$	0:0	$\frac{4}{3}:\frac{2}{3}$	0:2
$^1P_1$	0:0	$\frac{2}{3}:\frac{4}{3}$	$\frac{2}{3}:\frac{4}{3}$
$^3P_2$	$0:\frac{2}{5}$	$0:\frac{6}{5}$	$\frac{4}{3}:\frac{16}{15}$
$^3D_1$	$\frac{2}{3}:0$	$\frac{2}{3}:0$	$\frac{4}{15}:\frac{12}{5}$
$^3D_2$	0:0	$\frac{6}{5}:\frac{4}{5}$	$\frac{2}{5}:\frac{8}{5}$
$^1D_2$	0:0	$\frac{4}{5}:\frac{6}{5}$	$\frac{4}{5}:\frac{6}{5}$
$^3D_3$	$0:\frac{3}{7}$	$0:\frac{8}{7}$	$\frac{8}{5}:\frac{29}{35}$
$^3F_2$	$\frac{3}{5}:0$	$\frac{4}{5}:0$	$\frac{11}{35}:\frac{16}{7}$
$^3F_3$	0:0	$\frac{8}{7}:\frac{6}{7}$	$\frac{4}{7}:\frac{10}{7}$
$^1F_3$	0:0	$\frac{6}{7}:\frac{8}{7}$	$\frac{6}{7}:\frac{8}{7}$
$^3F_4$	$0:\frac{4}{9}$	$0:\frac{10}{9}$	$\frac{12}{7}:\frac{46}{63}$
$^3G_3$	$\frac{4}{7}:0$	$\frac{6}{7}:0$	$\frac{22}{63}:\frac{20}{9}$
$^3G_4$	0:0	$\frac{10}{9}:\frac{8}{9}$	$\frac{2}{3}:\frac{4}{3}$
$^1G_4$	0:0	$\frac{8}{9}:\frac{10}{9}$	$\frac{8}{9}:\frac{10}{9}$
$^3G_5$	$0:\frac{5}{11}$	$0:\frac{12}{11}$	$\frac{16}{9}:\frac{67}{99}$

where the summation runs over momentum, spin, and flavor. Above threshold (for $W>M_i+M_j$), Ω is complex. We decompose Ω_{nm} into a dynamical part (see [10]) that depends on the radial and orbital quantum numbers of the charmonium states and on the masses of D_i and D_j times the product recoupling matrix shown in Table II that expresses the spin dependence for each partial wave.

In each channel $^{2S+1}L_J$, the physical states correspond to the eigenvalues of

$$(\mathcal{H}_{c\bar{c}}+\Omega(W))\Psi=W\Psi. \qquad (5)$$

The real parts of the energy eigenvalues are the charmonium masses. Imaginary parts determine the widths of resonances above threshold. The eigenvalues also determine the mixing among $(c\bar{c})$ states and the overall fraction in the $(c\bar{c})$ sector.

To fix the (Coulomb+linear) charmonium potential,

$$V(r)=-\kappa/r+r/a^2, \qquad (6)$$

we adjust the strength of the linear term to reproduce the observed ψ'-ψ splitting, *after including all the effects of coupling to virtual decay channels*. Neglecting the influence of open charm gives $a=2.34$ GeV, $\kappa=0.52$, and a charmed-quark mass $m_c=1.84$ GeV. In the Cornell coupled-channel model, the virtual decay channels reduce the ψ'-ψ splitting by about 115 MeV, so the slope parameter has to be reduced to $a=1.97$ GeV.

The basic coupled-channel interaction (3) is spin independent, but the hyperfine splittings of D and D^*, D_s and D_s^*, induce spin-dependent forces that affect the charmonium states. These spin-dependent forces give rise to S-D mixing that contributes to the $\psi(3770)$ electronic width, for example,

TABLE III. Charmonium spectrum, including the influence of open-charm channels. All masses are in MeV. The penultimate column holds an estimate of the spin splitting due to tensor and spin-orbit forces in a single-channel potential model. The last column gives the spin splitting induced by communication with open-charm states, for an initially unsplit multiplet.

State	Mass	Centroid	Splitting (potential)	Splitting (induced)
1^1S_0	2979.9[a]	3067.6[b]	−90.5	+2.8
1^3S_1	3096.9[a]		+30.2	−0.9
1^3P_0	3415.3[a]		−114.9[e]	+5.9
1^3P_1	3510.5[a]	3525.3[c]	−11.6[e]	−2.0
1^1P_1	3525.3		+1.5[e]	+0.5
1^3P_2	3556.2[a]		−31.9[e]	−0.3
2^1S_0	3637.7[a]	3673.9[b]	−50.4	+15.7
2^3S_1	3686.0[a]		+16.8	−5.2
1^3D_1	3769.9[a,b]		−40	−39.9
1^3D_2	3830.6	(3815)[d]	0	−2.7
1^1D_2	3838.0		0	+4.2
1^3D_3	3868.3		+20	+19.0
2^3P_0	3931.9		−90	+10
2^3P_1	4007.5	3968[d]	−8	+28.4
2^1P_1	3968.0		0	−11.9
2^3P_2	3966.5		+25	−33.1

[a]Observed mass, from *Review of Particle Physics*, Ref. [13].
[b]Inputs to potential determination.
[c]Observed 1^3P_J centroid.
[d]Computed.
[e]Required to reproduce observed masses.

and are a source of additional spin splitting, shown in the rightmost column of Table III. To compute the induced splittings, we adjust the bare centroid of the spin-triplet states so that the physical centroid, after inclusion of coupled-channel effects, matches the value in the middle column of Table III. As expected, the shifts induced in the low-lying $1S$ and $1P$ levels are small. For the other known states in the $2S$ and $1D$ families, coupled-channel effects are noticeable and interesting.

In a simple potential picture, the $\eta_c'(2^1S_0)$ level lies below the $\psi'(2^3S_1)$ by the hyperfine splitting given by $M(\psi')-M(\eta_c')=32\pi\alpha_s|\Psi(0)|^2/9m_c^2$. Normalizing to the observed $1S$ hyperfine splitting, $M(J/\psi)-M(\eta_c)=117$ MeV, we would find

$$M(\psi')-M(\eta_c')=67 \text{ MeV}, \tag{7}$$

which is larger than the observed 48.3 ± 4.4 MeV, as is typical for potential-model calculations. The $2S$-induced shifts in Table III draw ψ' and η_c' closer by 20.9 MeV, substantially improving the agreement between theory and experiment. It is tempting to conclude that the ψ'-η_c' splitting reflects the influence of virtual decay channels.

We lack a comprehensive theory of spin splittings for $L>0$ states, and various potential-model schemes differ appreciably in their predictions. (See Table I of Ref. [12] for a variety of estimates.) For the $1P$ states, the spin splittings shown under Splitting (potential) in Table III are those required to reproduce the observed masses; they are not predictions. For the $1D$ and $2P$ levels, we have adopted as representative the spin splittings shown.

To reproduce the observed mass of the 1^3D_1 $\psi(3770)$, we shift the bare $1D$ centroid upward by 67.5 MeV. The other $1D$ masses are thus pegged to the observed $\psi(3770)$. In our model calculation, the coupling to open-charm channels increases the 1^3D_2-1^3D_1 splitting by about 20 MeV, but does not fully account for the observed 102 MeV separation between $X(3872)$ and $\psi(3770)$. It is noteworthy that the position of the $3^{--}1^3D_3$ level turns out to be very close to 3872 MeV. For the $2P$ levels, we have no experimental anchor, so we adjust the bare centroid so that the 2^1P_1 level lies at the centroid of the potential-model calculation. It is likely that we have more to learn about the influence of open-charm channels.

The 2^1P_1 level has been suggested [14] as an alternative assignment for $X(3872)$ because it has an allowed $\pi\pi$ transition to J/ψ and a hindered $M1$ radiative transition to the $1P$ levels. The coupled-channel calculation places this state nearly 100 MeV above $D\bar{D}^*$ threshold. As we shall see in quantitative detail presently, its allowed s-wave decay to $D^0\bar{D}^{*0}$ leads to an unacceptably large width, unless $X(3872)$ lies below the $D^0\bar{D}^{*0}$ threshold.

The wave functions that correspond to physical states are linear combinations of potential-model $c\bar{c}$ eigenstates plus admixtures of charmed-meson pairs. We record the charmonium content of states of interest in Table IV. The open-charm pieces have the spatial structure of bound states of charmed mesons, but they are not molecular charm states in the usual sense: they are virtual contributions for states below threshold, and—unlike ''deusons,'' for example [15]—they are not bound by one-pion exchange.

Expectations for radiative transitions. As Table IV shows, the physical charmonium states are not pure potential-model eigenstates. To compute the $E1$ radiative transition rates, we must take into account both the standard $(c\bar{c})\to(c\bar{c})\gamma$ transitions and the transitions between (virtual) decay channels in the initial and final states. Details of the calculational procedure are given in Sec. IV B of Ref. [11].

Our expectations for $E1$ transition rates among spin-triplet levels are shown in Table V. There we show both the rates calculated between single-channel potential-model eigenstates (in italics) and the rates that result from the Cornell coupled-channel model, to indicate the influence of the open-charm channels. The model reproduces the trends of transitions to and from the χ_c states in broad outline. Not surprisingly, the single-channel values roughly track those calculated by Barnes and Godfrey in their potential [12]. For these low-lying states, the mixing through open-charm channels results in a mild reduction of the rates.

We show the 1^3D_1 transition rates at the mass of $\psi(3770)$ and at the predicted 1^3D_1 centroid, 3815 MeV. For the $\psi(3770)$, with its total width of about 24 MeV, the $1^3D_1(3770)\to\chi_{c0}\gamma(338)$ transition might someday be observable with a branching fraction of 1%.

TABLE IV. Charmonium content of states near flavor threshold. The wave function Ψ takes account of mixing induced through open charm-anticharm channels. Unmixed potential-model eigenstates are denoted by $|n^{2s+1}L_J\rangle$. The coefficient of the dominant eigenstate is chosen real and positive. The $1S$, $1P$, $2S$, and 1^3D_1 states are evaluated at their physical masses. The remaining $1D$ and $2P$ states are considered at the masses in Table III. We also show the 1^3D_2, 1^3D_3, and 2^1P_1 states at the mass of $X(3872)$. $\mathcal{Z}_{c\bar{c}}$ represents the $(c\bar{c})$ probability fraction of each state.

$\Psi(1^1S_0) = 0.986|1^1S_0\rangle - 0.042|2^1S_0\rangle - 0.008|3^1S_0\rangle - 0.002|4^1S_0\rangle - 0.001|5^1S_0\rangle$; $\mathcal{Z}_{c\bar{c}} = 0.974$

$\Psi(1^3S_1) = 0.983|1^3S_1\rangle - 0.050|2^3S_1\rangle - 0.009|3^3S_1\rangle - 0.003|4^3S_1\rangle - 0.001|5^3S_1\rangle$; $\mathcal{Z}_{c\bar{c}} = 0.968$

$\Psi(1^3P_0) = 0.919|1^3P_0\rangle - 0.067|2^3P_0\rangle - 0.014|3^3P_0\rangle - 0.005|4^3P_0\rangle - 0.002|5^3P_0\rangle$; $\mathcal{Z}_{c\bar{c}} = 0.850$

$\Psi(1^3P_1) = 0.914|1^3P_1\rangle - 0.075|2^3P_1\rangle - 0.015|3^3P_1\rangle - 0.005|4^3P_1\rangle - 0.002|5^3P_1\rangle$; $\mathcal{Z}_{c\bar{c}} = 0.841$

$\Psi(1^1P_1) = 0.918|1^1P_1\rangle - 0.077|2^1P_1\rangle - 0.015|3^1P_1\rangle - 0.005|4^1P_1\rangle - 0.002|5^1P_1\rangle$; $\mathcal{Z}_{c\bar{c}} = 0.845$

$\Psi(1^3P_2) = 0.920|1^3P_2\rangle - 0.080|2^3P_2\rangle - 0.015|3^3P_2\rangle - 0.005|4^3P_2\rangle - 0.002|5^3P_2\rangle - 0.002|1^3F_2\rangle$; $\mathcal{Z}_{c\bar{c}} = 0.854$

$\Psi(2^1S_0) = 0.087|1^1S_0\rangle + 0.883|2^1S_0\rangle - 0.060|3^1S_0\rangle - 0.016|4^1S_0\rangle - 0.007|5^1S_0\rangle - 0.003|6^1S_0\rangle$; $\mathcal{Z}_{c\bar{c}} = 0.791$

$\Psi(2^3S_1) = 0.103|1^3S_1\rangle + 0.838|2^3S_1\rangle - 0.085|3^3S_1\rangle - 0.017|4^3S_1\rangle - 0.007|5^3S_1\rangle - 0.002|6^3D_1\rangle + 0.040|1^3D_1\rangle - 0.008|2^3D_1\rangle$; $\mathcal{Z}_{c\bar{c}} = 0.723$

$\Psi(1^3D_1) = 0.694|1^3D_1\rangle + 0.097e^{0.935i\pi}|2^3D_1\rangle + 0.008e^{-0.668i\pi}|3^3D_1\rangle + 0.006e^{0.904i\pi}|4^3D_1\rangle + 0.013e^{0.742i\pi}|1^3S_1\rangle + 0.168e^{0.805i\pi}|2^3S_1\rangle + 0.014e^{0.866i\pi}|3^3S_1\rangle + 0.012e^{-0.229i\pi}|4^3S_1\rangle + 0.001e^{0.278i\pi}|5^3S_1\rangle + 0.001e^{-0.267i\pi}|6^3S_1\rangle$; $\mathcal{Z}_{c\bar{c}} = 0.520$

$\Psi(1^3D_2) = 0.754|1^3D_2\rangle - 0.084|2^3D_2\rangle - 0.011|3^3D_2\rangle - 0.006|4^3D_2\rangle$; $\mathcal{Z}_{c\bar{c}} = 0.576$

$\Psi(1^1D_2) = 0.770|1^1D_2\rangle - 0.083|2^1D_2\rangle - 0.012|3^1D_2\rangle - 0.006|4^1D_2\rangle$; $\mathcal{Z}_{c\bar{c}} = 0.600$

$\Psi(1^3D_3) = 0.812|1^3D_3\rangle + 0.086e^{0.990i\pi}|2^3D_3\rangle + 0.013e^{-0.969i\pi}|3^3D_3\rangle + 0.007e^{0.980i\pi}|4^3D_3\rangle + 0.016e^{0.848i\pi}|1^3G_3\rangle + 0.003e^{-0.291i\pi}|2^3G_3\rangle$; $\mathcal{Z}_{c\bar{c}} = 0.667$

$\Psi(2^3P_0) = 0.040e^{-0.454i\pi}|1^3P_0\rangle + 0.532|2^3P_0\rangle + 0.024e^{-0.889i\pi}|3^3P_0\rangle + 0.010e^{0.867i\pi}|4^3P_0\rangle + 0.006e^{-0.976i\pi}|5^3P_0\rangle$; $\mathcal{Z}_{c\bar{c}} = 0.286$

$\Psi(2^3P_1) = 0.218e^{-0.456i\pi}|1^3P_1\rangle + 0.821|2^3P_1\rangle + 0.058e^{0.516i\pi}|3^3P_1\rangle + 0.032e^{0.976i\pi}|4^3P_1\rangle + 0.008e^{0.986i\pi}|5^3P_1\rangle$; $\mathcal{Z}_{c\bar{c}} = 0.726$

$\Psi(2^1P_1) = 0.216e^{-0.226i\pi}|1^1P_1\rangle + 0.852|2^1P_1\rangle + 0.079e^{0.780i\pi}|3^1P_1\rangle + 0.023e^{-0.890i\pi}|4^1P_1\rangle 0.007e^{0.985i\pi}|5^1P_1\rangle$; $\mathcal{Z}_{c\bar{c}} = 0.883$

$\Psi(2^3P_2) = 0.234e^{-0.046i\pi}|1^3P_2\rangle + 0.754|2^3P_2\rangle + 0.097e^{0.876i\pi}|3^3P_2\rangle + 0.016e^{-0.743i\pi}|4^3P_2\rangle 0.007e^{0.898i\pi}|5^3P_2\rangle + 0.370e^{0.775i\pi}|1^3F_2\rangle + 0.035e^{-0.317i\pi}|2^3F_2\rangle + 0.002e^{0.097i\pi}|3^3F_2\rangle$; $\mathcal{Z}_{c\bar{c}} = 0.771$

$M = 3872$ MeV: $\Psi(1^3D_2) = 0.596|1^3D_2\rangle - 0.108|2^3D_2\rangle - 0.004|3^3D_2\rangle - 0.006|4^3D_2\rangle$; $\mathcal{Z}_{c\bar{c}} = 0.367$

$M = 3872$ MeV: $\Psi(1^3D_3) = 0.813|1^3D_3\rangle + 0.089e^{0.989i\pi}|2^3D_3\rangle + 0.013e^{-0.965i\pi}|3^3D_3\rangle + 0.007e^{0.978i\pi}|4^3D_3\rangle + 0.017e^{0.837i\pi}|1^3G_3\rangle + 0.003e^{-0.305i\pi}|2^3G_3\rangle$; $\mathcal{Z}_{c\bar{c}} = 0.669$

$M = 3872$ MeV: $\Psi(2^1P_1) = 0.134e^{-0.004i\pi}|1^1P_1\rangle + 0.374|2^1P_1\rangle + 0.035e^{0.993i\pi}|3^1P_1\rangle + 0.003e^{-0.981i\pi}|4^1P_1\rangle + 0.004e^{0.996i\pi}|5^1P_1\rangle$; $\mathcal{Z}_{c\bar{c}} = 0.159$

For the 1^3D_2 and 1^3D_3 levels, we have computed the radiative decay rates at the predicted 1^3D_1 centroid, 3815 MeV, at the mass calculated for the states (3831 MeV and 3868 MeV, respectively), and at the mass of $X(3872)$. We will compare the partial widths for the $\chi_{c1}\gamma(344)$ and $\chi_{c2}\gamma(303)$ with the expected $\pi^+\pi^- J/\psi$ and open-charm decay rates presently.

We have evaluated the radiative decay rates for the 2^3P_J levels at the calculated centroid and at the predicted mass, where that is displaced appreciably from the centroid. We shall see below that all of these rates are small compared to the expected open-charm decay rates.

Expectations for hadronic transitions. The Beijing Spectrometer (BES) observation [16] of a branching fraction $\mathcal{B}(\psi(3770) \to \pi^+\pi^- J/\psi) = (0.59 \pm 0.26 \pm 0.16)\%$ would imply a hadronic cascade rate $\Gamma(1^3D_1 \to \pi\pi J/\psi) \approx 210 \pm 130$ keV, considerably larger than the 45 keV, inferred [17] from older data, which we took as normalization in Ref. [2]. By the Wigner-Eckart theorem for $E1$-$E1$ transitions, all the $1^3D_J \to \pi\pi J/\psi$ rates should be equal (for degenerate ^3D_J states), so the higher BES normalization would increase $\Gamma(1^3D_2 \to \pi\pi J/\psi)$ to hundreds of keV, as remarked by Barnes and Godfrey [12]. Combined with our estimate that $\Gamma(1^3D_2(3872) \to \gamma\chi_{c1}) \approx 207$ keV, the larger $\pi\pi J/\psi$ rate relaxes somewhat—but does not eliminate—the tension between the $^3D_2$ assignment for X and the Belle bound in Eq. (2).

The BES rate, which is based on a handful of events, is challenged by a CLEO-*c* limit [9], $\mathcal{B}(\psi(3770) \to \pi^+\pi^- J/\psi) < 0.26\%$ at 90% C.L. Both experiments are accumulating larger data samples that should improve our knowledge of this important normalization.

III. DECAYS INTO OPEN CHARM

The calculated partial widths for decays of charmonium states into open charm appear in Table VI. Experience [10] teaches us that once the position of a resonance is given, the

TABLE V. Calculated and observed rates for $E1$ radiative transitions among charmonium levels. *Values in italics* result if the influence of open-charm channels is not included.

Transition (γ energy in MeV)	Partial width (keV)	
	Computed	Measured
$\chi_{c0}\to J/\psi\gamma(303)$	*113*→107	119 ± 19[a]
$\chi_{c1}\to J/\psi\gamma(390)$	*228*→216	291 ± 48[a]
$\chi_{c2}\to J/\psi\gamma(429)$	*300*→287	426 ± 51[a]
$\psi'\to\chi_{c2}\gamma(129)$	*23*→23	27 ± 4[b]
$\psi'\to\chi_{c1}\gamma(172)$	*33*→32	27 ± 3[b]
$\psi'\to\chi_{c0}\gamma(261)$	*36*→38	27 ± 3[b]
$1^3D_1(3770)\to\chi_{c2}\gamma(208)$	*3.2*→3.9	
$1^3D_1(3770)\to\chi_{c1}\gamma(251)$	*183*→59	
$1^3D_1(3770)\to\chi_{c0}\gamma(338)$	*254*→225	
$1^3D_1(3815)\to\chi_{c2}\gamma(250)$	*5.5*→6.8	
$1^3D_1(3815)\to\chi_{c1}\gamma(293)$	*128*→120	
$1^3D_1(3815)\to\chi_{c0}\gamma(379)$	*344*→371	
$1^3D_2(3815)\to\chi_{c2}\gamma(251)$	*50*→40	
$1^3D_2(3815)\to\chi_{c1}\gamma(293)$	*230*→191	
$1^3D_2(3831)\to\chi_{c2}\gamma(266)$	*59*→45	
$1^3D_2(3831)\to\chi_{c1}\gamma(308)$	*264*→212	
$1^3D_2(3872)\to\chi_{c2}\gamma(303)$	*85*→45	
$1^3D_2(3872)\to\chi_{c1}\gamma(344)$	*362*→207	
$1^3D_3(3815)\to\chi_{c2}\gamma(251)$	*199*→179	
$1^3D_3(3868)\to\chi_{c2}\gamma(303)$	*329*→286	
$1^3D_3(3872)\to\chi_{c2}\gamma(304)$	*341*→299	
$2^3P_0(3933)\to J/\psi\gamma(747)$	*95*→19	
$2^3P_0(3933)\to\psi'\gamma(239)$	*127*→38	
$2^3P_0(3933)\to\psi(3770)\gamma(160)$	*59*→11	
$2^3P_0(3968)\to J/\psi\gamma(775)$	*110*→77	
$2^3P_0(3968)\to\psi'\gamma(272)$	*180*→155	
$2^3P_0(3968)\to\psi(3770)\gamma(193)$	*101*→43	
$2^3P_1(3968)\to J/\psi\gamma(775)$	*110*→68	
$2^3P_1(3968)\to\psi'\gamma(272)$	*180*→102	
$2^3P_1(3968)\to\psi(3770)\gamma(193)$	*25*→5	
$2^3P_1(3968)\to1^3D_2(3815)\gamma(150)$	*37*→1.8	
$2^3P_1(3968)\to1^3D_2(3831)\gamma(135)$	*25*→0.25	
$2^3P_1(3968)\to1^3D_2(3872)\gamma(95)$	*10*→0.23	
$2^3P_1(4012)\to J/\psi\gamma(811)$	*132*→94	
$2^3P_1(4012)\to\psi'\gamma(313)$	*260*→151	
$2^3P_1(4012)\to\psi(3770)\gamma(235)$	*43*→11	
$2^3P_2(3968)\to J/\psi\gamma(775)$	*110*→19	
$2^3P_2(3968)\to\psi'\gamma(272)$	*180*→314	
$2^3P_2(3968)\to\psi(3770)\gamma(193)$	*1.0*→1.4	
$2^3P_2(3968)\to1^3D_2(3815)\gamma(150)$	*7.4*→18	
$2^3P_2(3968)\to1^3D_2(3835)\gamma(131)$	*5*→12	
$2^3P_2(3968)\to1^3D_2(3872)\gamma(95)$	*1.9*→3.4	
$2^3P_2(3968)\to1^3D_3(3815)\gamma(150)$	*41*→82	
$2^3P_2(3968)\to1^3D_3(3868)\gamma(99)$	*12*→26	
$2^3P_2(3968)\to1^3D_3(3872)\gamma(95)$	*11*→23	

[a]Derived from the 2003 "unchecked fit" of Ref. [13].
[b]Branching fractions from CLEO via Skwarnicki [9].

coupled-channel formalism yields reasonable predictions for the other resonance properties. The 1^3D_1 state $\psi''(3770)$, which lies some 40 MeV above the charm threshold, offers an important benchmark: we compute $\Gamma(\psi''(3770)\to D\bar{D})=20.1$ MeV, to be compared with the Particle Data Group's fitted value of 23.6 ± 2.7 MeV [13]. The variation of the 1^3D_1 width with mass is shown in the top left panel of Fig. 1.

Barnes and Godfrey [12] have estimated the decays of several of the charmonium states into open charm, using the $^3P_0$ model of $q\bar{q}$ production first applied above charm threshold by the Orsay group [18]. They did not carry out a coupled-channel analysis, and so did not determine the composition of the physical states, but their estimates of open-charm decay rates can be read against ours as a rough assessment of model dependence.

The long-standing expectation that the 1^3D_2 and 1^1D_2 levels would be narrow followed from the presumption that these unnatural parity states should lie between the $D\bar{D}$ and $D\bar{D}^*$ thresholds, and could not decay into open charm. At 3872 MeV, both states can decay into $D^0\bar{D}^{*0}$, but the partial widths (Table VI) are quite small. We show the variation of the 1^3D_2 partial width with mass in the middle left panel of Fig. 1; over the region of interest, it does not threaten the Belle bound, $\Gamma(X(3872))<2.3$ MeV. The range of values is quite similar to the range estimated for $\Gamma(1^3D_2\to\pi\pi J/\psi)$, so we expect roughly comparable branching fractions for decays into $D^0\bar{D}^{*0}$ and $\pi^+\pi^-J/\psi$. If $X(3872)$ does turn out to be the 1^3D_2 level, we expect $M(1^1D_2)=3880$ MeV and $\Gamma(1^1D_2\to D^0\bar{D}^{*0})\approx1.7$ MeV.

The natural-parity 1^3D_3 state can decay into $D\bar{D}$, but its f-wave decay is suppressed by the centrifugal barrier factor, so the partial width is less than 1 MeV at a mass of 3872 MeV. Although estimates of the hadronic cascade transitions are uncertain, the numbers in hand lead us to expect $\Gamma(1^3D_3\to\pi^+\pi^-J/\psi)\lesssim1/4\Gamma(1^3D_3\to D\bar{D})$, whereas $\Gamma(1^3D_3\to\gamma\chi_{c2})\approx1/3\Gamma(1^3D_3\to D\bar{D})$, if $X(3872)$ is identified as 1^3D_3. The variation of $\Gamma(1^3D_3\to D\bar{D})$ with mass is shown in the bottom left panel of Fig. 1. Note that if 1^3D_3 is not to be identified with $X(3872)$, *it may still be discovered as a narrow* $D\bar{D}$ *resonance*, up to a mass of about 4000 MeV.

In their study of $B^+\to K^+\psi(3770)$ decays, the Belle Collaboration [19] has set 90% C.L. upper limits on the transition $B^+\to K^+X(3872)$, followed by $X(3872)\to D\bar{D}$. Their limits imply that

$$\mathcal{B}(X(3872)\to D^0\bar{D}^0)\lesssim4\mathcal{B}(X\to\pi^+\pi^-J/\psi),$$

$$\mathcal{B}(X(3872)\to D^+D^-)\lesssim3\mathcal{B}(X\to\pi^+\pi^-J/\psi). \qquad (8)$$

This constraint is already intriguingly close to the level at which we would expect to see $1^3D_3\to D\bar{D}$.

The constraint on the total width of $X(3872)$ raises more of a challenge for the 2^1P_1 candidate, whose s-wave decay to $D^0\bar{D}^{*0}$ rises dramatically from threshold, as shown in the

TABLE VI. Partial widths for decays of charmonium states into open charm, computed in the Cornell coupled-channel model. All masses and widths are in MeV. Only significant partial widths are tabulated, and ''total'' refers to the sum of open-charm decays. Properties of the candidate states for $X(3872)$ and their partners are evaluated at 3872 MeV and also at the potential-model centroid for each state. Decays occur with orbital angular momentum ℓ. For $D\bar{D}^*$ modes, the sum of $D\bar{D}^*$ and $\bar{D}D^*$ is always implied.

State	Mass	ℓ	Channel	Width	Total width
1^3D_1	3770	1	$D^0\bar{D}^0$	11.8	20.1
			D^+D^-	8.3	
1^3D_2	3815	-	—	0	0
1^3D_2	3872	1	$D^0\bar{D}^{*0}$	0.045	0.045
1^1D_2	3815	-	—	0	0
1^1D_2	3872	1	$D^0\bar{D}^{*0}$	0.030	0.030
1^1D_2	3880	1	$D^0\bar{D}^{*0}$	1.7	1.7
1^3D_3	3872	3	$D^0\bar{D}^0$	0.47	0.86
			D^+D^-	0.39	
1^3D_3	3902	3	$D^0\bar{D}^0$	0.84	1.56
			D^+D^-	0.72	
2^3P_0	3872	0	$D^0\bar{D}^0$	27	59
			D^+D^-	32	
2^3P_0	3930	0	$D^0\bar{D}^0$	5.0	12.4
			D^+D^-	7.4	
2^3P_0	3968	0	$D^0\bar{D}^0$	0.27	41.1
			D^+D^-	0.85	
			$D_s\bar{D}_s$	40	
2^3P_1	3872	0	$D^0\bar{D}^{*0}$	20.9	20.9
2^3P_1	3968	0	$D^0\bar{D}^{*0}$	71.4	150.3
			D^+D^{*-}	78.9	
2^1P_1	3871.6	0	$D^0\bar{D}^{*0}$	4.28	4.28
2^1P_1	3968	0	$D^0\bar{D}^{*0}$	35.5	74.7
			D^+D^{*-}	39.2	
2^3P_2	3872	2	$D^0\bar{D}^0$	1.63	3.05
			D^+D^-	1.42	
2^3P_2	3968	2	$D^0\bar{D}^0$	4.4	13.4
			D^+D^-	4.2	
			$D^0\bar{D}^{*0}$	2.57	
			D^+D^{*-}	2.16	
1^3F_2	4054	2	$D^0\bar{D}^0$	46	155
			D^+D^-	45	
			$D_s\bar{D}_s$	4	
			$D^0\bar{D}^{*0}$	31	
			D^+D^{*-}	29	
1^3F_3	4054	2	$D^0\bar{D}^{*0}$	44.9	87.5
			D^+D^{*-}	42.6	
1^1F_3	4054	2	$D^0\bar{D}^{*0}$	32.2	66.4
			D^+D^{*-}	30.8	
1^3F_4	4054	4	$D^0\bar{D}^0$	1.96	4.88
			D^+D^-	1.78	
			$D^0\bar{D}^{*0}$	0.62	
			D^+D^{*-}	0.50	

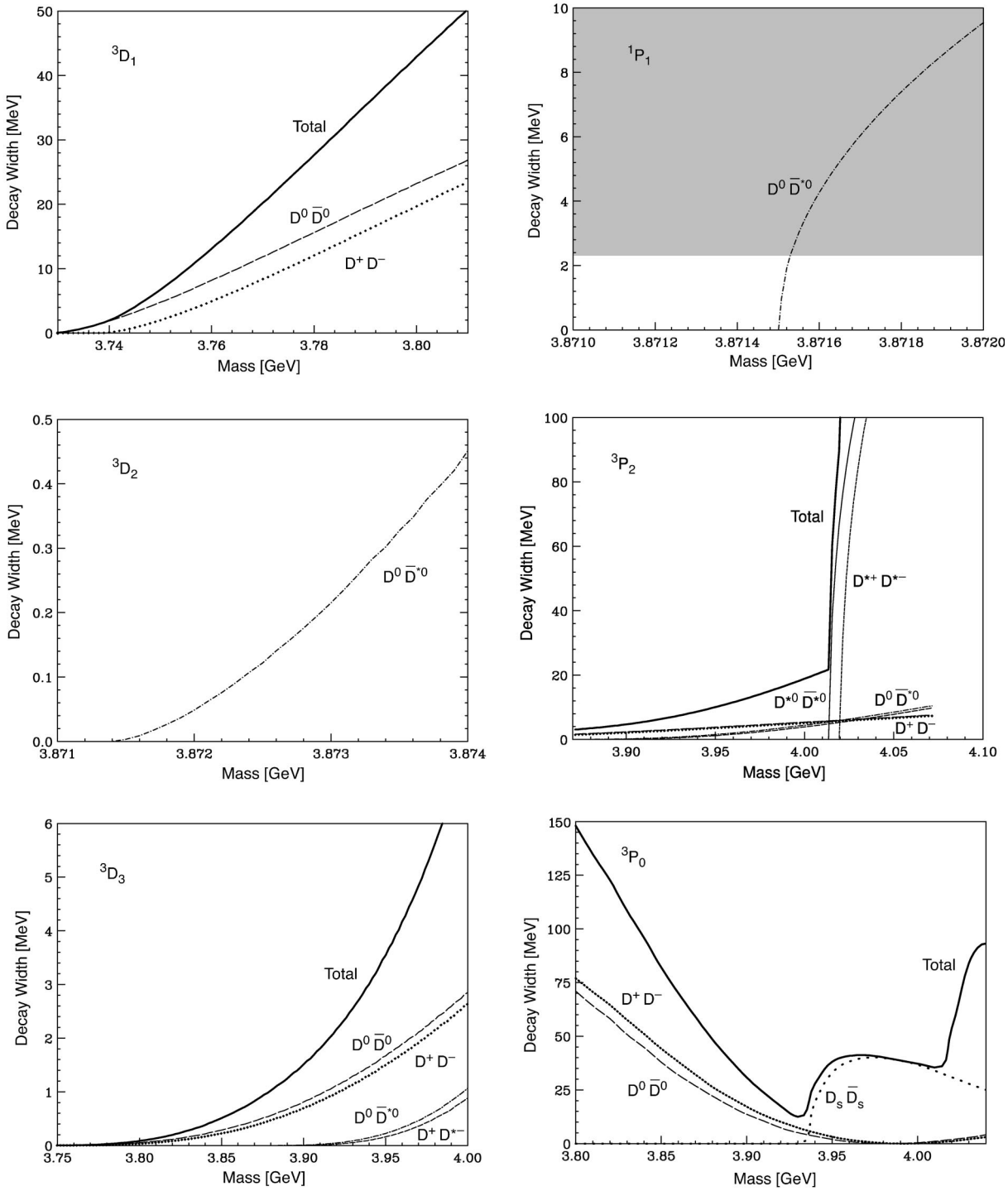

FIG. 1. Partial and total widths near threshold for decay of charmonium states into open charm, computed in the Cornell coupled-channel model. Long dashes: $D^0\bar{D}^0$. Dots: D^+D^-. Dot-dashes: $D^0\bar{D}^{*0}$. Dashes: D^+D^{*-}. Thin line: $D^{*0}\bar{D}^{*0}$. Short dashes: $D^{*+}D^{*-}$. Widely spaced dots: $D_s\bar{D}_s$. Thick line: sum of open-charm channels. Belle's 90% C.L. upper limit [3], $\Gamma(X(3872))<2.3$ MeV, is indicated on the $^1P_1$ window. For $D\bar{D}^*$ modes, the sum of $D\bar{D}^*$ and $\bar{D}D^*$ is always implied.

top right panel of Fig. 1. Within the current uncertainty (3871.7 ± 0.6 MeV) in the mass of X, the issue cannot be settled, but the 2^1P_1 interpretation is viable only if X lies below $D^0\bar{D}^{*0}$ threshold. If a light 2^1P_1 does turn out to be $X(3872)$, then its 2^3P_J partners should lie nearby. In that case, they should be visible as relatively narrow charm-anticharm resonances. At 3872 MeV, we estimate $\Gamma(2^3P_1\rightarrow D\bar{D}^*)\approx 21$ MeV and $\Gamma(2^3P_2\rightarrow D\bar{D})\approx 3$ MeV. The

middle right panel in Fig. 1 shows that the 2^3P_2 level remains relatively narrow up to the opening of the $D^*\bar{D}^*$ threshold.

The 2^3P_0 state is an interesting special case, as illustrated in the bottom right panel of Fig. 1. Through the interplay of nodes in the radial wave function, form-factor effects, and the opening of new channels, $\Gamma(2^3P_0 \to D\bar{D})$ decreases from $\approx$60 MeV at 3872 MeV to about 12 MeV near 3930 MeV. The total width for decay to open charm then rises in steps as $M(2^3P_0)$ increases through the $D_s\bar{D}_s$ and $D^*\bar{D}^*$ thresholds. To estimate the competing annihilation decay rate, we scale $\Gamma(2^3P_0 \to gg \to \text{hadrons}) \approx \Gamma(1^3P_0 \to gg \to \text{hadrons}) \times |R'_{2P}(0)|^2/|R'_{1P}(0)|^2$, where $R'(0)$ is the derivative of the radial wave function at the origin. This yields $\Gamma(2^3P_0 \to gg \to \text{hadrons}) \approx 1.36 \times 10.6\ \text{MeV} = 14.4\ \text{MeV}$ [13], an estimate that should probably be reduced by the $|2^3P_0\rangle$ fraction of the physical 2^3P_0 state.

We call attention to one more candidate for a narrow resonance of charmed mesons: The 1^3F_4 level remains narrow ($\Gamma(1^3F_4 \to \text{charm}) \lesssim 5$ MeV) up to the $D^*\bar{D}^*$ threshold. Its allowed decays into $D\bar{D}$ and $D\bar{D}^*$ are inhibited by $\ell = 4$ barrier factors, whereas the $D^*\bar{D}^*$ channel is reached by $\ell = 2$.

IV. FOR THE FUTURE

On the experimental front, the first order of business is to establish the nature of $X(3872)$. Determining the spin-parity of X will winnow the field of candidates. The charmonium interpretation and its prominent rivals require that $X(3872)$ be a neutral isoscalar. Are there charged partners? A search for $X(3872) \to \pi^0\pi^0 J/\psi$ will be highly informative. As Barnes and Godfrey [12] have remarked, observing a significant $\pi^0\pi^0 J/\psi$ signal establishes that X is odd under charge conjugation. Voloshin has commented [20] that the ratio $\mathcal{R}_0 \equiv \Gamma(X \to \pi^0\pi^0 J/\psi)/\Gamma(X \to \pi^+\pi^- J/\psi)$ measures the dipion isospin. Writing $\Gamma_I \equiv \Gamma(X \to (\pi^+\pi^-)_I J/\psi)$, we see that $\mathcal{R}_0 = 1/2/(1+\Gamma_1/\Gamma_0)$, up to kinematic corrections. Deviations from $\mathcal{R}_0 = 1/2$ signal the isospin-violating decay of an isoscalar or the isospin-conserving decay of an isovector. Radiative decay rates and the prompt (as opposed to B-decay) production fraction will provide important guidance. Other diagnostics of a general nature have been discussed in Refs. [12,14,21,22].

Within the charmonium framework, $X(3872)$ is most naturally interpreted as the 1^3D_2 or 1^3D_3 level, both of which have< allowed decays into $\pi\pi J/\psi$. The $2^{--}1^3D_2$ state is forbidden by parity conservation to decay into $D\bar{D}$ but has a modest $D^0\bar{D}^{*0}$ partial width for masses near 3872 MeV. Although the uncertain $\pi\pi J/\psi$ partial width makes it difficult to estimate relative branching ratios, the decay $X(3872) \to \chi_{c1}\gamma(344)$ should show itself if X is indeed 1^3D_2. The $\chi_{c2}\gamma(303)$ line should be seen with about 1/4 the strength of $\chi_{c1}\gamma(344)$. In our coupled-channel calculation, the 1^3D_2 mass is about 41 MeV lower than the observed 3872 MeV. In contrast, the computed 1^3D_3 mass is quite close to 3872 MeV, and 1^3D_3 does not have an $E1$ transition to $\chi_{c1}\gamma(344)$. The dominant decay of the $3^{--}1^3D_3$ state should be into $D\bar{D}$; a small branching fraction for the $\pi\pi J/\psi$ discovery mode would imply a large production rate. One radiative transition should be observable, with $\Gamma(X(3872) \to \chi_{c2}\gamma(303)) \gtrsim \Gamma(X(3872) \to \pi^+\pi^- J/\psi)$. We underscore the importance of searching for the $\chi_{c1}\gamma(344)$ and $\chi_{c2}\gamma(303)$ lines.

Beyond pinning down the character of $X(3872)$, experiments can search for additional narrow charmonium states in radiative and hadronic transitions to lower-lying $c\bar{c}$ levels, as we emphasized in Ref. [2], and in neutral combinations of charmed mesons and anticharmed mesons. The coupled-channel analysis presented in this paper sets up specific targets.

On the theoretical front, we need a more complete understanding of the production of the charmonium states in B decays and by direct hadronic production, including the influence of open-charm channels. Understanding of the production mechanisms for molecular charm or $c\bar{c}g$ hybrid states is much more primitive. We need to improve the theoretical understanding of hadronic cascades among charmonium states, including the influence of open-charm channels. The comparison of charmonium transitions with their upsilon counterparts should be informative. The analysis we have carried out can be extended to the $b\bar{b}$ system, where it may be possible to see discrete threshold-region states in direct hadronic production. Because the Cornell coupled channel model is only an approximation to QCD, it would be highly desirable to compare its predictions with those of a coupled-channel analysis of the $^3P_0$ model of quark pair production. Ultimately, extending lattice QCD calculations into the flavor-threshold region should give a firmer basis for predictions.

In addition to the $1\ ^1P_1\ h_c$, the now-established $2\ ^1S_0\ \eta'_c$, and the long-sought $1\ ^1D_2\ \eta_{c2}$ and $1\ ^3D_2\ \psi_2$ states, discrete charmonium levels are to be found as narrow charm-anticharm structures in the flavor-threshold region. The most likely candidates correspond to the $1\ ^3D_3$, $2\ ^3P_2$, and $1\ ^3F_4$ levels. If $X(3872)$ is indeed a charmonium state—the $^3D_2$ and $^3D_3$ assignments seem most promising—then identifying that state anchors the mass scale. If $X(3872)$ is not charmonium, then all the charmonium levels remain to be discovered. Finding these states—and establishing their masses, widths, and production rates—will lead us into new terrain.

ACKNOWLEDGMENTS

We thank Steve Olsen, J. D. Jackson, Stephen Godfrey, Gerry Bauer, Brad Abbott, Vivek Jain, Sheldon Stone, and participants in the Quarkonium Working Group's Second Workshop on Heavy Quarkonium for inspiring discussions. K.L.'s research was supported by the Department of Energy under Grant No. DE-FG02-91ER40676. Fermilab is operated by Universities Research Association Inc. under Contract No. DE-AC02-76CH03000 with the U.S. Department of Energy.

[1] Belle Collaboration, S. K. Choi *et al.*, Phys. Rev. Lett. **89**, 102001 (2002); **89**, 129901(E) (2002).
[2] E. J. Eichten, K. Lane, and C. Quigg, Phys. Rev. Lett. **89**, 162002 (2002).
[3] Belle Collaboration, S. K. Choi *et al.*, Phys. Rev. Lett. **91**, 262001 (2003).
[4] CDF II Collaboration, D. Acosta *et al.*, hep-ex/0312021.
[5] DØ Collaboration, DØ Note 4334, 2004, URL http://www-d0.fnal.gov/Run2Physics/ckm/Moriond_2003/X_conf_note_v9.ps.
[6] CLEO Collaboration, D. M. Asner, hep-ex/0312058.
[7] BABAR Collaboration, G. Wagner, hep-ex/0305083.
[8] Belle Collaboration, K. Abe *et al.*, hep-ex/0306015.
[9] T. Skwarnicki, hep-ph/0311243.
[10] E. Eichten, K. Gottfried, T. Kinoshita, K. D. Lane, and T.-M. Yan, Phys. Rev. D **17**, 3090 (1978); **21**, 313(E) (1980).
[11] E. Eichten, K. Gottfried, T. Kinoshita, K. D. Lane, and T.-M. Yan, Phys. Rev. D **21**, 203 (1980).
[12] T. Barnes and S. Godfrey, hep-ph/0311162.
[13] Particle Data Group, K. Hagiwara *et al.*, Phys. Rev. D **66**, 010001 (2002), and 2003 off-year partial update, URL http://pdg.lbl.gov.
[14] S. Pakvasa and M. Suzuki, Phys. Lett. B **579**, 67 (2004).
[15] N. A. Törnqvist, hep-ph/0402237.
[16] BES Collaboration, J. Z. Bai *et al.*, hep-ex/0307028.
[17] E. J. Eichten and C. Quigg, Phys. Rev. D **49**, 5845 (1994).
[18] A. Le Yaouanc, L. Oliver, O. Pène, and J. C. Raynal, Phys. Lett. **71B**, 397 (1977).
[19] Belle Collaboration, K. Abe *et al.*, hep-ex/0307061.
[20] M. Voloshin (private communication).
[21] F. E. Close and P. R. Page, Phys. Lett. B **578**, 119 (2004).
[22] F. E. Close and S. Godfrey, Phys. Lett. B **574**, 210 (2003).